R. & M. No. 3351

MINISTRY OF AVIATION

AERONAUTICAL RESEARCH COUNCIL
REPORTS AND MEMORANDA

The Use of Surface Pitot Tubes as Skin-Friction Meters at Supersonic Speeds

By K. G. SMITH, L. GAUDET and K. G. WINTER

LONDON: HER MAJESTY'S STATIONERY OFFICE
1964
PRICE 15*s.* 0*d.* NET

The Use of Surface Pitot Tubes as Skin-Friction Meters at Supersonic Speeds

By K. G. Smith, L. Gaudet and K. G. Winter

Communicated by the Deputy Controller Aircraft (Research and Development), Ministry of Aviation

*Reports and Memoranda No. 3351**

June, 1962

Summary.

Experiments have been made, in supersonic turbulent boundary layers, on a simple type of surface pitot tube, formed by cementing a piece of razor blade over a static-pressure hole. This type of surface pitot tube has great practical advantages, as surface-shear measurements may be made on any model designed for pressure measurements.

A calibration curve, which is sensibly independent of Mach number, has been obtained for the dependence of the pressure rise at the pitot tube on the surface shear, both terms being made non-dimensional. Examples are included of the use of surface pitot tubes on two models. The models were a delta wing and a biconvex cone and the tests covered a range of Mach numbers, Reynolds numbers and model incidence.

LIST OF CONTENTS

* Replaces R.A.E. Report No. Aero. 2665—A.R.C. 24,179.

LIST OF TABLES

LIST OF ILLUSTRATIONS

---

1. *Introduction.*

The interest in recent years in efficient flight at supersonic speeds has led to the development of shapes with low wave drag as exemplified by the work of Lord and Brebner[1]. For such shapes the skin-friction contribution to the drag is significant. For example, the tests of Ormerod and Sprinks[2] on an uncambered delta wing of aspect ratio 2/3 and centreline thickness-chord ratio of 8·43% show that in the wind tunnel the skin friction contributes some 60% of the total drag at zero lift. This contribution can apparently be estimated well by flat-plate turbulent-skin-friction formulae. However, at zero incidence the pressure distribution on the model of Ref. 2 is relatively simple and the three-dimensional effects on the boundary layer are small. For wings at incidence and with camber, the pressure gradients and three-dimensional effects may be expected to play a larger part in determining the skin friction.

Reviews of methods of calculating three-dimensional boundary layers have been given by Sears[3], Moore[4], and Cooke and Hall[5]. These reviews, however, deal almost exclusively with laminar boundary layers, whereas the boundary layer on a typical aircraft will be turbulent over most of the surface. For turbulent boundary layers, as in two dimensions, recourse must be had to empirical formulae for the surface shearing stress. The shearing stress is taken as the same as for two-dimensional flow along the external streamlines with further assumptions necessary for the cross-flow shearing stress. Even for two-dimensional flow there is little information on the effect of pressure gradient on surface shearing stress, and it was thus thought well worth while to attempt to measure the distribution of shearing stress on slender wings.

In Section 2 various methods of measuring skin friction are discussed. Of these methods the most straightforward is the use of surface pitot tubes. Hool[17] has shown that a surface pitot tube can

be produced in a simple manner by attaching a piece of razor blade to a surface provided with a flush hole such that the chamfer of the blade edge overlaps the hole. This technique has been adopted in the work described herein.

In Section 3 earlier work on surface pitot tubes is reviewed. In Sections 4 and 5 the method adopted for obtaining a calibration curve and the results obtained are discussed.

In Section 6 the application of surface pitot tubes to the measurement of skin friction on models in a wind tunnel is described, with estimates of accuracy. The results of preliminary tests on two models are given in Sections 7 and 8.

The results which have been obtained so far show that surface pitot tubes are usable in turbulent boundary layers in supersonic flow with some possible reservations as to the effects of pressure gradient.

2. *Methods of Measuring the Surface Shearing Stress in Boundary Layers.*

In order that the aim of measuring the distribution of shearing stress over a wing should be a practicable experiment a method was required which would neither require specialised equipment and techniques nor depend upon a multiplicity of readings for the evaluation of a single point. Methods such as that of Schubauer and Klebanoff[6] using hot wires to measure the distribution of shearing stress through the boundary layer, or methods based on application of the momentum integral equations or on the velocity profile close to the wall were therefore not considered. The three methods considered are discussed below.

(i) *Floating surface element.*

This technique, in which the force on a small, detached portion of the surface is measured, is the only direct method of measuring skin friction. The method was first used by Kempf[7], whose measurements for Reynolds numbers greater than 100 million are still the only values available in this range. Dhawan[8] showed that the technique could be used successfully at transonic and supersonic speeds, and Smith and Walker[9] recently made some very careful measurements in incompressible flow at Reynolds numbers up to 43 million, using an improved type of measuring device.

As well as being the only absolute method, this is also the most accurate method, Smith and Walker[9] claiming an accuracy of 2 per cent. This method has the serious disadvantage that in a pressure gradient, the pressure difference across the floating element will contribute a force, which can only be estimated, and which may be of the same order as the total shearing force on the surface of the element. In zero pressure gradient, however, this method provides a very accurate standard which can be used to check other methods of measuring skin friction. However, either the installation of a number of units in a model or the repeated installation of a single unit in various positions would clearly be a prohibitive problem.

(ii) *Heated surface element.*

Ludwieg[10] developed a method of determining skin friction by measuring the heat transfer from a small, locally insulated, heated portion of the surface. Liepmann and Skinner[11] showed that the method could be simplified by using a heated wire embedded in the surface, and Diaconis[12] has extended Ludwieg's theoretical analysis to compressible flow. This method was used by Ludwieg and Tillman[13] to obtain an empirical law for the local skin-friction coefficient in incompressible flows with pressure gradients. The only limitation on the use of this method is that the heated

portion of the surface be so small that its thermal boundary layer lies within the laminar sublayer of the velocity boundary layer. The method is quick, as only two measurements are required, the temperature of the heated surface under two different rates of heat transfer, one of which may be conveniently chosen as zero heat transfer. A slight disadvantage is the time taken for the surface to reach thermal equilibrium with its surroundings, which may be considerable. The use of this method would demand special models with provision for the necessary wiring.

(iii) *Surface pitot tube.*

Surface pitot tubes were first used by Stanton, Marshall and Bryant[14] to show the existence of a laminar sublayer in turbulent pipe flow. Fage and Falkner[15] used surface pitot tubes to measure the distribution of skin friction on a two-dimensional aerofoil. In recent years renewed interest in surface pitot tubes has been aroused by Preston[16], who, on the basis of Ludwieg and Tillman's experiments, suggested that circular pitot tubes could be used to measure skin friction, instead of the rather delicate flat pitot tubes used by Stanton. Shortly afterwards Hool[17] devised a very simple type of surface pitot tube, consisting of a small piece of a razor blade soldered over a pressure hole in the surface, thus converting a static-pressure hole into a surface pitot tube. The assumption behind the use of surface pitot tubes is that the mean velocity profile of a turbulent boundary layer, in the region near the wall, is determined solely by the shearing stress at the wall and the properties of the fluid. Ludwieg and Tillman[13] have shown this to be true independent of pressure gradients for incompressible flows and Monaghan and Cooke[18] have shown independence for supersonic Mach numbers with zero pressure gradients, provided that the properties of the fluid were evaluated at the temperature of the surface. Despite the lack of accurate measurements on a compressible boundary layer in a pressure gradient, it appears reasonable in the present state of knowledge to assume that the velocity profile is determined solely by the wall shearing stress and the properties of the fluid so that the same calibration should apply to geometrically similar surface pitot tubes at all speeds.

From the foregoing it can be seen that both the heat-transfer and surface-pitot methods provide means of obtaining the skin friction in a completely unknown boundary layer from local measurements only. These each have advantages and disadvantages. The heat-transfer method makes a less restrictive assumption about the velocity profile in the boundary layer than the surface-pitot-tube method, but is rather less accurate, as the signal is proportional to the 1/3 power of the shearing stress, instead of the 8/7 power for surface pitot tubes.

Following the idea of Hool the use of a portion of razor blade to produce a surface pitot tube has tremendous practical advantages. On any model where provision has been made for measuring pressures the surface shear can be measured, without any additional instrumentation, by converting the pressure holes into surface pitot tubes. Strictly a measure of surface temperature is also required but this can usually be estimated with sufficient accuracy.

On practical grounds alone a study of such devices at supersonic speeds was warranted, with the aim, if possible, of obtaining a calibration relating the surface shear and pitot pressure rise independently of Mach number.

3. *Previous Work on Surface Pitot Tubes.*

After the work of Stanton *et al*[14], and Fage and Falkner[15], Taylor[19] analysed their results, and showed that a unique non-dimensional correlation could be obtained. He also carried out further experiments to extend the range of the calibration curve. The correlation suggested by Taylor

involved the idea of the 'effective centre' of the pitot tube. Later Preston[16] suggested a more simple correlation by making both the surface shear and pressure rise non-dimensional thus obtaining the equation*

$$\frac{\rho_w h^2 \tau_w}{\mu_w{}^2} = f\left(\frac{\rho_w h^2 \Delta P}{\mu_w{}^2}\right), \tag{1}$$

where

τ_w = wall shearing stress,

ρ_w = density at wall,

μ_w = viscosity at wall,

h = height of surface pitot tube,

ΔP = pressure difference between surface pitot pressure and local static pressure.

This equation is rather more useful than Taylor's correlation as the wall shearing stress is given directly in terms of the other variables. The function f will be different for geometrically different surface pitot tubes. A good survey of work up to 1954 has been given by Trilling and Hakkinen[20], together with an attempt to predict theoretically the form of the function f. Work subsequent to this paper is discussed below.

Preston [16] gave the calibration curve

$$\frac{\rho_w h^2 \tau_w}{\mu_w{}^2} = 0{\cdot}0478\left(\frac{\rho_w h^2 \Delta P}{\mu_w{}^2}\right)^{0{\cdot}875}, \tag{2}$$

from tests in fully developed pipe flow at low speeds, using circular pitot tubes, for the range $2{\cdot}5 \times 10^5 < \rho_w h^2 \Delta P/\mu_w{}^2 < 10^7$. Shortly afterwards Relf, Pankhurst and Walker[21] obtained the calibration

$$\frac{\rho_w h^2 \tau_w}{\mu_w{}^2} = 0{\cdot}0543\left(\frac{\rho_w h^2 \Delta P}{\mu_w{}^2}\right)^{0{\cdot}875}, \tag{3}$$

for a turbulent boundary layer on a flat plate, over the range $5 \times 10^5 < \rho_w h^2 \Delta P/\mu_w{}^2 < 5 \times 10^7$. Hsu[22] verified Preston's original calibration for boundary layers in adverse pressure gradients, using the Ludwieg-Tillman formula for skin friction. Smith and Walker[9] calibrated surface pitot tubes in a turbulent boundary layer by measuring the shearing stress with a floating element, and obtained the relationship

$$\frac{\rho_w h^2 \tau_w}{\mu_w{}^2} = 0{\cdot}0511\left(\frac{\rho_w h^2 \Delta P}{\mu_w{}^2}\right)^{0{\cdot}877}, \tag{4}$$

over the range $4 \times 10^5 < \rho_w h^2 \Delta P/\mu_w{}^2 < 10^7$. This agrees with (3) within about 4% over the common range of applicability. For a laminar boundary layer the only available results are those by Relf *et al*[21], who give

$$\frac{\rho_w h^2 \tau_w}{\mu_w{}^2} = 2{\cdot}25\left(\frac{\rho_w h^2 \Delta P}{\mu_w{}^2}\right)^{1/2}, \tag{5}$$

* It might be remarked that the L.H.S. of equation (1) is the square of a Reynolds number using friction velocity and that the parameter on the R.H.S. is half the square of a Reynolds number using the velocity indicated by the surface pitot tube.

over the range $10^5 < \rho_w h^2 \Delta P/\mu_w^2 < 4 \times 10^6$. For compressible boundary layers, the only results using circular pitot tubes are those of Fenter and Stalmach[23], who used a different correlation from (1). For incompressible flow a surface-pitot-tube velocity, U_s, may be defined by the relationship

$$\Delta P = \tfrac{1}{2}\rho_w U_s^2. \tag{6}$$

Then (1) is equivalent to

$$\frac{\rho_w h^2 \tau_w}{\mu_w^2} = f_1\left(\frac{\rho_w h U_s}{\mu_w}\right), \tag{7}$$

where the function f_1 in (7) is related to the function f in (1). For compressible flow Fenter and Stalmach generalised (7) to

$$\frac{\rho_w h^2 \tau_w}{\mu_w^2} = f_1(\alpha), \tag{8}$$

where

$$\alpha = \frac{\rho_w h U_1}{\mu_w}\frac{1}{\sqrt{\sigma}}\sin^{-1}\left(\frac{U_s\sqrt{\sigma}}{U_1}\right), \tag{9}$$

where U_s is the velocity measured by the surface pitot tube, i.e. the velocity deduced from the ratio of surface pitot pressure to local static pressure, assuming constant stagnation temperature throughout the boundary layer. In (9)

$$\sigma = \frac{\gamma-1}{2}M_1^2\Big/\left(1+\frac{\gamma-1}{2}M_1^2\right),$$

where U_1 and M_1 are the velocity and Mach number, respectively, of the external flow. It is clear that (7) and (8) are identical for incompressible flow ($M_1 \to 0$). Fenter and Stalmach[23] measured the shearing stress at the wall using a floating element, and tested a series of surface pitot tubes over a wide range of tube diameters, Mach numbers and Reynolds numbers, and obtained a satisfactory correlation of the form (8). For incompressible flow the correlation they obtained is within about 6% of that given by (3).

For flat surface pitot tubes information is rather scarcer. Hool[17] calibrated a series of tubes in laminar duct flow, and obtained the correlation

$$\frac{\rho_w h^2 \tau_w}{\mu_w^2} = 0{\cdot}741\left(\frac{\rho_w h^2 \Delta P}{\mu_w^2}\right)^{5/8}, \tag{10}$$

over the range $15 < \rho_w h^2 \Delta P/\mu_w^2 < 2000$. Bradshaw and Gregory[24] made tests on a series of surface pitot tubes in laminar duct flow over the range $1{\cdot}2 < \rho_w h^2 \Delta P/\mu_w^2 < 200$, and in fully developed turbulent duct flow over the range $1{\cdot}2 < \rho_w h^2 \Delta P/\mu_w^2 < 10^7$. An analytic expression for the calibration curve is not given, but it is shown that different calibration curves must be used in laminar and turbulent flows. Over the range of overlap with Hool's results the calibrations agree within about 5%. For compressible flow, results using flat surface pitot tubes were obtained by Abarbanel, Hakkinen and Trilling[25]. They used a flattened pitot tube resting against the surface of a flat plate in the transition region of a boundary layer at subsonic speeds, and in laminar and fully turbulent boundary layers at supersonic speeds. For the subsonic boundary layer, and the laminar supersonic boundary layer, the correlation obtained was

$$\frac{\rho_w h^2 \tau_w}{\mu_w^2} = 0{\cdot}54\left(\frac{\rho_w h^2 \Delta P}{\mu_w^2}\right)^{3/5}, \tag{11}$$

over the range $1{\cdot}4 \times 10^2 < \rho_w h^2 \Delta P/\mu_w{}^2 < 5 \times 10^3$. For the turbulent supersonic boundary layer the correlation obtained was

$$\frac{\rho_w h^2 \tau_w}{\mu_w{}^2} = 0{\cdot}211 \left(\frac{\rho_w h^2 \Delta P}{\mu_w{}^2}\right)^{3/4}, \tag{12}$$

over the range $6 \times 10^3 < \rho_w h^2 \Delta P/\mu_w{}^2 < 1{\cdot}4 \times 10^5$.

Theoretical attempts to predict the calibration to be used for surface pitot tubes have mostly been unsuccessful. For circular pitot tubes both Hsu[22] for incompressible flow, and Fenter and Stalmach[23] for compressible flow assumed that the pressure recorded by the surface pitot tube was the mean pitot pressure over the portion of the boundary layer occupied by the pitot tube. They showed that to sufficient accuracy the mean pressure was the same as the pressure at the centre of the pitot tube, and that the experimental results were in satisfactory agreement with the theoretical results. For a linear velocity profile, as occurs in laminar boundary layers, Preston[16] suggested that the calibration should be

$$\frac{\rho_w h^2 \tau_w}{\mu_w{}^2} = 2\sqrt{2} \left(\frac{\rho_w h^2 \Delta P}{\mu_w{}^2}\right)^{1/2}, \tag{13}$$

which is within about 25% of the curve given by Relf *et al*[21] for a laminar boundary layer.

For flat surface pitot tubes, Thom[26] performed a numerical calculation of the flow around a two-dimensional surface pitot tube at very low Reynolds numbers (Stokes flow regime). From his results he deduced the calibration

$$\frac{\rho_w h^2 \tau_w}{\mu_w{}^2} = \tfrac{1}{2} \frac{\rho_w h^2 \Delta P}{\mu_w{}^2}, \tag{14}$$

which is of the same form as the calibration obtained by Taylor[19], but with a different numerical coefficient (0·50 instead of 0·82). For turbulent boundary layers Trilling and Hakkinen[20] assumed that the effect of the surface pitot tube could be treated as a linear perturbation to the boundary-layer flow. When the surface pitot tube lay within the linear velocity profile in the boundary layer they predicted a correlation of the form

$$\frac{\rho_w h^2 \tau_w}{\mu_w{}^2} = A \left(\frac{\rho_w h^2 \Delta P}{\mu_w{}^2}\right)^{3/5}. \tag{15}$$

This analysis was extended by Abarbanel *et al*[25] to the case where the surface pitot tube projected well beyond the linear velocity profile, giving a correlation of the form

$$\frac{\rho_w h^2 \tau_w}{\mu_w{}^2} = B \left(\frac{\rho_w h^2 \Delta P}{\mu_w{}^2}\right)^{6/7}. \tag{16}$$

Gadd[27] has investigated the effect of separation upstream of a step in a flow with linear velocity profile and obtained the calibration

$$\frac{\rho_w h^2 \tau_w}{\mu_w{}^2} = C \left(\frac{\rho_w h^2 \Delta P}{\mu_w{}^2}\right)^{3/4}. \tag{17}$$

By appropriate choice of constants these calibrations can be made to fit experimental results over a fairly wide range of the variables.

As none of this work covers calibration of surface pitot tubes of the type considered in this report over the Mach number and Reynolds number ranges required, the experiments described in Sections 4 and 5 were undertaken.

4. *Method of Calibration.*

The type of surface pitot tube used consisted of a piece of razor blade cemented to the surface, with its leading edge immediately above the leading edge of a circular pressure hole in the surface, as shown in Fig. 1. Most of the razor blade above the sharp leading edge was ground away, as indicated, in order to reduce as much as possible the disturbance to the boundary layer. The grinding does not affect the calibration. The height h, from the leading edge to the surface, was varied by varying the amount of cement under the razor blade, or, for the largest values, by inserting a piece of paper or thin cardboard packing between the razor blade and the surface, as shown in Fig. 2. The surface pitot tubes were not all exactly geometrically similar, the aspect ratio of the orifice varying from about 100 down to 15. However, it is believed that these values are large enough for the flow in the neighbourhood of the tube to be two dimensional in character, and that the aspect ratio does not enter as an additional parameter.

The surface pitot tubes were calibrated in the turbulent boundary layer on the flat sidewall of two supersonic wind tunnels at R.A.E., Bedford. In order to examine the effect of varying Reynolds number, measurements were made in the 9 in. × 8 in. Tunnel at a Mach number of 2, for Reynolds numbers between 2 million and 8 million per foot. To examine the effect of varying Mach number, the 13 in. × 13 in. Tunnel was used at atmospheric total pressure, for Mach numbers between 1·8 and 2·7. Boundary-layer traverses were made, using a flattened pitot tube, and pressures were recorded using surface pitot tubes of several different heights in each tunnel.

After several unfruitful attempts to determine the skin friction by using von Kármán's momentum integral equation, the following method was adopted. The mean skin-friction coefficient, C_F, for a two-dimensional incompressible turbulent boundary layer of effective length x is given by the two formulae (*see* Monaghan and Johnson[28])

$$C_F = \frac{2\theta}{x}, \tag{18}$$

$$C_F = 0{\cdot}46\,[\log_{10} Re_x]^{-2{\cdot}6}. \tag{19}$$

Hence if θ and the Reynolds number per foot are known, a value of x may be obtained which gives the same value of C_F from both (18) and (19). Then the local skin-friction coefficient, c_f, may be calculated from the formula (*see* Monaghan[29])

$$c_f = 0{\cdot}288\,[\log_{10} Re_x]^{-2{\cdot}45}. \tag{20}$$

For compressible flow the 'intermediate enthalpy' forms (Ref. 29) of (19) and (20) are used. C_F, c_f and Re_x are replaced by $C_F{}^*$, $c_f{}^*$ and $Re_x{}^*$, with the relations

$$C_F{}^* = \frac{\rho_1}{\rho^*} C_F,$$

$$c_f{}^* = \frac{\rho_1}{\rho^*} c_f,$$

$$Re_x{}^* = \frac{\rho^*}{\rho_1}\frac{\mu_1}{\mu^*} Re_x,$$

where ρ_1 and μ_1 are the free-stream density and viscosity, respectively, and ρ^* and μ^* are the density and viscosity corresponding to the intermediate temperature T^*, with

$$T^* = T_1 + 0{\cdot}5(T_w - T_1) + 0{\cdot}22(T_r - T_1),$$

where T_1 is the free-stream temperature, T_w is the wall temperature, and T_r is the recovery temperature, i.e. the wall temperature for zero heat transfer. The wall temperature was evaluated by assuming that there was no heat transfer and that a recovery factor of 0·89 could be taken. Both these assumptions can be justified. The airswept surfaces of the sidewalls of both wind tunnels are covered with a layer of resinous material about 0·01 in. thick. As the recovery temperature at a Mach number of 2·7 is only 20°C below the total temperature (for total temperatures around 20°C) the heat-transfer rate will be very small. The tunnels were run for several minutes before taking readings to enable the surface temperature to reach equilibrium. The effects of variations in the recovery factor are negligible. For example, changing the recovery factor from 0·89 to 0·88 changes the surface temperature, and hence the density and viscosity, by less than $\frac{1}{2}\%$.

The assumption implicit in the foregoing is that the local skin-friction coefficient is determined solely by the Reynolds number based on momentum thickness, and is unaffected by pressure gradients or three-dimensional effects. In both wind tunnels pressure gradients in the vicinity of the measuring points were small. In the 9 in. × 8 in. Tunnel the measuring point is preceded by a length of about a foot of uniform flow, and in the 13 in. × 13 in. Tunnel the maximum divergence of the nozzle wall in the supersonic portion of the nozzle is only 10°, so that three-dimensional effects should be small in both tunnels, and the values of c_f deduced should be close to the correct values. The characteristics of the boundary layers measured are summarised in Tables 1 and 2. As a check on the reliability of the deduced skin-friction coefficient the velocity profiles for a few of the boundary-layer traverses are plotted in Figs. 3 and 4 in the 'law of the wall' form,

$$\frac{u}{u_\tau} = f\left(\frac{yu_\tau}{\nu_w}\right), \tag{21}$$

where

$$u_\tau = (\tau_w/\rho_w)^{1/2},$$

$$\nu_w = \mu_w/\rho_w,$$

and u is the velocity in the boundary layer at a point distant y from the wall. Over the centre portion of the boundary layer the profiles are close to the form

$$\frac{u}{u_\tau} = 5{\cdot}0 \log_{10}\left(\frac{yu_\tau}{\nu_w}\right) + 7{\cdot}15$$

as suggested by Smith and Walker[9] for incompressible flow. There is some variation with Reynolds number, as also obtained by Smith and Walker. Tests in the 9 in. × 8 in. Tunnel in fact covered almost the same Reynolds number range as Smith and Walker's tests, and the straight-line portions of two of their profiles are also shown in Fig. 3, where it can be seen that the results agree very well with the results obtained here.

The surface pitot tubes were placed at several longitudinal positions on the centreline of the sidewall in the 9 in. × 8 in. Tunnel, and at one position on the centreline and at a position $3\frac{1}{2}$ inches above this on the sidewall of the 13 in. × 13 in. Tunnel. It was expected that the boundary layer would have different characteristics at these different positions, but Tables 1 and 2 show that the differences were quite small. The calibration obtained for the surface pitot tubes, in the form

$$\frac{\rho_w h^2 \tau_w}{\mu_w{}^2} = f\left(\frac{\rho_w h^2 \Delta P}{\mu_w{}^2}\right), \tag{22}$$

is shown in Fig. 5.

5. *Results and Discussion.*

5.1. *Results for Unyawed Surface Pitot Tubes.*

The calibration results obtained are shown in Fig. 5. The least-squares line through the points is

$$\frac{\rho_w h^2 \tau_w}{\mu_w{}^2} = 0{\cdot}207 \left(\frac{\rho_w h^2 \Delta P}{\mu_w{}^2} \right)^{0{\cdot}764} . \tag{23}$$

Previous results for flat surface pitot tubes over the range of $\rho_w h^2 \Delta P / \mu_w{}^2$ covered in these tests by Bradshaw and Gregory[24] for incompressible flow in a duct, and by Abarbanel *et al*[25] for a turbulent boundary layer at supersonic speeds, are also shown in Fig. 5. The results obtained here agree well with the measurements of Abarbanel *et al*, {cf. equation (23) with equation (12)} but it should be pointed out that Abarbanel *et al* state that the flattened pitot tube used by them as a surface pitot tube did not have its lower surface touching the wall. If the lower surface had been touching the wall the measured pressure rise, ΔP, would have been smaller, and this would have brought the results into even closer agreement. The results obtained here do not agree very well with those of Bradshaw and Gregory. This discrepancy may be due to slight differences in the geometry of the tubes, differences in velocity profiles in duct and boundary-layer flow, or a genuine Mach number effect. It seems likely that there is a genuine Mach number effect since the presence of the surface pitot tube will induce a small local separation. The pressure rise in the region of separation will be influenced by shock waves at supersonic speeds.*

The least-squares line {equation (23)} should not be used beyond the range of tests covered here. Extension of the results to smaller values of $\rho_w h^2 \tau_w / \mu_w{}^2$ would be difficult, as it would involve either using smaller heights h, or tests at lower values of ρ_w and τ_w obtained by operating at reduced Reynolds number. In both of these cases accurate measurements would be made more difficult. Extension to larger values of $\rho_w h^2 \tau_w / \mu_w{}^2$, on the other hand, may be made simply by increasing h, which does not lead to any loss of accuracy.

In this connection some measurements by Stevens[30, 31] of the pressure coefficients on steps of various heights in a turbulent boundary layer at several Mach numbers have been analysed. The boundary layer for these tests was roughly of the same thickness as that used to calibrate the surface pitot tubes, and the step heights varied from less than 1/10 to over $\frac{1}{2}$ of the boundary-layer thickness, the smallest step height being about 5 times the largest surface-pitot-tube height. The skin-friction coefficients in the undisturbed boundary layer at the step positions were estimated using flat-plate formulae for turbulent boundary layers. The results are compared with the surface-pitot-tube calibration in Fig. 6, using the correlation

$$\frac{c_p}{c_f} = g \left(\frac{h u_\tau}{\nu_w} \right),$$

where c_p is the mean pressure coefficient on the front face of the step, and c_f is the skin-friction coefficient for the undisturbed boundary layer. It is easily seen that this correlation is equivalent to (1). With this correlation Stevens' results collapse on to a unique curve independent of Mach number or step height. This curve does not overlap the range covered by the surface-pitot correlation and differs from the curve calculated from equation (23). It does, however, fair into the surface-pitot

* Work subsequent to that reported here has shown that different calibration curves are, in fact, obtained for subsonic and supersonic speeds, with a transitional region for Mach numbers between about 0·8 and 1·5.

line. This indicates that a unique correlation exists up to quite large values of the height h. The relationship given by equation (23) is clearly not valid for values of hu_τ/ν exceeding 100. Provisionally the extension indicated by the results for steps might be used for larger values of hu_τ/ν.

5.2. *Effects of Yaw on Surface Pitot Tubes.*

Before surface pitot tubes can be used in three-dimensional boundary layers the effects of yaw on the pressure measured by a surface pitot tube need to be investigated. The only measurements to date have been those of Sigalla in an unpublished report, which have been described by Granville and Boxall[32]. These were made using a circular pitot tube at low speeds, and the results may be quite different for flat surface pitot tubes at supersonic speeds. The effects of yawing a surface pitot tube up to 30° were studied in the 9 in. × 8 in. Tunnel. These results may be presented in two ways. In Fig. 7 the results for one particular height of surface pitot tube, 0·0040 in., are plotted as

$$\frac{\Delta P_\beta}{\Delta P_0} = g(\beta), \tag{24}$$

where ΔP_β is the pressure rise above local static pressure recorded by the surface pitot tube at an angle of yaw β, ΔP_0 being the pressure rise at zero yaw. The results of Sigalla are also included. The alternative method of plotting is shown in Fig. 8, as

$$\frac{\tau_\beta}{\tau_0} = h(\beta), \tag{25}$$

where τ_β is the shearing stress at an angle of yaw β, deduced from (23), and τ_0 is the shearing stress obtained for zero yaw, i.e. the true shearing stress.

There are two simple physical ideas which enable us to deduce the forms of the functions $g(\beta)$ and $h(\beta)$ in (24) and (25). If it is assumed, following Fenter and Stalmach[23], that the pressure rise, ΔP, recorded by the surface pitot tube corresponds to a velocity U in the boundary layer, such that

$$\Delta P = \tfrac{1}{2}\rho U^2,$$

then for yawed surface pitot tubes, assuming that the relevant velocity is the velocity normal to the leading edge of the surface pitot tube, the relation

$$U_\beta = U_0 \cos\beta,$$

is obtained, which leads to

$$\frac{\Delta P_\beta}{\Delta P_0} = \cos^2\beta. \tag{26}$$

The curve given by (26) is shown in Fig. 7, where it can be seen to agree extremely well with all results up to yaw angles of 15°, and agrees with the high Reynolds number tests in the 9 in. × 8 in. Tunnel at all yaw angles. The results of Sigalla, and those for large yaw angles at low Reynolds numbers in the 9 in. × 8 in. Tunnel do not lie on the curve, but are within about 5% of it up to 30° yaw. An alternative assumption is that the pressure rise recorded by the surface pitot tube is that corresponding to the shearing stress normal to the leading edge. This gives immediately

$$\frac{\tau_\beta}{\tau_0} = \cos\beta. \tag{27}$$

The curve given by (27) is shown in Fig. 8, where it can be seen that it only agrees with the low Reynolds number tests in the 9 in. × 8 in. Tunnel, all other points lying well away from the curve,

except at very small angles of yaw. Although neither (26) nor (27) give a complete correlation for the effects of yaw, it is suggested that (26) should be used if it is desired to correct the measured pressure rise to the value it would have for an unyawed surface pitot tube, assuming that the direction of the skin friction on the surface is known, for example from oil-flow tests.

It should be made clear that this experiment on yawing a surface pitot tube in a two-dimensional boundary layer does not necessarily demonstrate its behaviour in a three-dimensional boundary layer in which the direction of flow will vary with the distance from the surface. Further work on this is desirable but will require extensive investigation of the characteristics of a three-dimensional boundary layer.

From Fig. 8 it should be noted that provided the normal to the leading edge of the surface pitot tube is within about 15° of the direction of the skin friction, the value of skin friction deduced from the calibration curve will be within about 5% of the true value.

5.3. *Interference between Surface Pitot Tubes.*

In order to determine how close the type of surface pitot tube considered here could be spaced streamwise without interference, measurements were made downstream of a surface pitot tube of height 0·0046 in. in the 9 in. × 8 in. Tunnel. It was found that neither the static pressure measured $1\frac{1}{2}$ in. downstream nor the surface pitot pressure measured 2 in. downstream were measurably altered. These distances are approximately two and three boundary-layer thicknesses, respectively. It was not possible to obtain any measurements at closer spacings than these, or on surface pitot tubes spaced spanwise, so that a lower limit to the spacing for negligible interference cannot be quoted. However, the spacings given should be sufficient for most purposes.

5.4. *Accuracy of Calibration.*

It is difficult to give precise estimates of the accuracy of the calibration curve due to uncertainty about the exact value of shearing stress. However, the accuracy of the remaining quantities in equation (23) may be estimated readily. The pressure difference ΔP was measured directly between the surface pitot tube and a neighbouring static-pressure hole to an accuracy of 0·001 in. Hg. As the lowest value of ΔP recorded was 0·25 in. Hg, the error in ΔP is not more than 0·4%. The static pressure was measured with an accuracy better than 1%. The estimated surface temperature is probably correct to about 3°C, or 1%. Hence ρ_w will be accurate to 2%, and μ_w to 1%. The height h is measured optically to an accuracy of about 0·0004 in., which gives an error in h varying from 30% for $h = 0{\cdot}0014$ in. to 4% for $h = 0{\cdot}0109$ in. Thus the error in $\rho_w h^2/\mu_w^2$ will range from 64% for $h = 0{\cdot}0014$ in. to 12% for $h = 0{\cdot}0109$ in. Hence the accuracy of the calibration curve is different over different portions of it. Rewriting (23) as

$$\tau_w = 0{\cdot}207(\Delta P)^{0{\cdot}764}\,(\rho_w h^2/\mu_w^2)^{-0{\cdot}236},$$

then the possible error in the constant 0·207, ignoring possible errors in τ_w, will be 15% for $h = 0{\cdot}0014$ in., and 3% for $h = 0{\cdot}0109$ in. If the error in τ_w is taken to be, say, 10%, then the accuracy of the calibration curve would be 25% near $\rho_w h^2 \Delta P/\mu_w^2 = 400$, and 13% for $\rho_w h^2 \Delta P/\mu_w^2 = 10^6$.

It is seen that the major inaccuracy of the calibration curve arises from errors in measuring h. The accuracy might be improved if a different way of measuring were used, such as a replica technique.

6. *Measurements of Skin Friction on Models—Method and Accuracy.*

To obtain an estimate of the accuracy obtainable from surface pitot tubes, the case of a typical model in the 8 ft × 8 ft Tunnel at R.A.E., Bedford, will be considered.

In general there will be pressure gradients on the model, and hence the pressure rise ΔP cannot be recorded directly, unless the model has been extensively pressure plotted in order to determine the isobars, in which case the surface pitot pressure may be measured relative to the static pressure anywhere on the same isobar. For tests in the 8 ft × 8 ft Wind Tunnel the following procedure has been adopted. The static pressures, P_S, are measured at a series of points on the model in one test. The static-pressure holes are converted into surface pitot tubes by cementing pieces of razor blade over them (*see* Fig. 1), and the test is repeated to give the surface pitot pressures, P_P, at the same points on the model surface. In general the tunnel total pressure for the two tests is not the same, so that the pressure rise ΔP is not equal to $P_P - P_S$. We assume that small variations in Reynolds number have an insignificant effect on the pressure coefficients, so that corrected static pressures, P_S', are obtained by multiplying P_S by the ratio of the total pressures. Then we have

$$\Delta P = P_P - P_S'. \tag{28}$$

The local Mach number is obtained from the ratio of static pressure to total pressure, assuming isentropic flow around the model (a reasonable assumption for slender configurations at moderate angles of incidence). The surface temperature, T_w, is obtained from the local Mach number, assuming a recovery factor of 0·89. The surface density, ρ_w, and viscosity, μ_w, may then be obtained. Thus all the quantities needed to evaluate $\rho_w h^2 \Delta P/\mu_w{}^2$, and hence $\rho_w h^2 \tau_w/\mu_w{}^2$ and τ_w are known.

To assess the accuracy of this procedure consider an example when the local Mach number is 2 with $c_f = 0{\cdot}0016$ at a Reynolds number per foot of 2 million and consider the surface pitot-pressure rise which would be measured by a tube of height 0·005 in. The various quantities involved are

$$\tau_w = 0{\cdot}648 \text{ lb/ft}^2,$$

$$\frac{\rho_w h^2}{\mu_w{}^2} = 202{\cdot}4 \text{ ft}^2/\text{lb},$$

hence

$$\frac{\rho_w h^2 \tau_w}{\mu_w{}^2} = 131{\cdot}1,$$

and from (23)

$$\frac{\rho_w h^2 \Delta P}{\mu_w{}^2} = 4{,}600,$$

giving

$$\Delta P = 22{\cdot}7 \text{ lb/ft}^2,$$

$$= 0{\cdot}33 \text{ in. Hg}.$$

Also

$$P_S = 2{\cdot}05 \text{ in. Hg}.$$

The pressures P_S and P_P are recorded to an accuracy of 0·02 in. Hg*, or about 1%. Half this error is reading error, and half zero error. Hence the accuracy of ΔP is 0·04 in. Hg, or about 12%. The error in Mach number is about 0·006, which gives a negligible error in T_w and μ_w. Hence the

* Subsequent to the tests discussed here the reading accuracy of the manometers has been improved to 0·005 in. Hg.

error in ρ_w is about 1%. The height h is measured optically, and an accuracy of about 0·0004 in. is obtainable, or about 8% in this case. Hence the accuracy of $\rho_w h^2/\mu_w{}^2$ is about 17%. From (23) the calibration curve may be written

$$\tau_w = 0{\cdot}207(\Delta P)^{0{\cdot}764}(\rho_w h^2/\mu_w{}^2)^{-0{\cdot}236}.$$

Hence the accuracy of τ_w is, ignoring possible errors in the calibration curve,

$$0{\cdot}764 \times 12 + 0{\cdot}236 \times 17 \doteqdot 13\%.$$

It is clear from this that the major factor in the accuracy of obtaining τ_w is the pressure rise ΔP. For example, at the same Mach number, but with a local skin-friction coefficient of 0·004, and a Reynolds number of 4 million per foot, the pressure rise is about 1·4 in. Hg, which is measurable to an accuracy of about 3%. Hence the error in τ_w is

$$0{\cdot}764 \times 3 + 0{\cdot}236 \times 17 \doteqdot 6\%.$$

On the other hand, for the same Reynolds number and skin-friction coefficient, but at a Mach number of 2·8, the pressure rise is about 0·12 in. Hg, which can only be measured to an accuracy of about 33%. Also the static pressure can only be measured to about 2%, so that the accuracy of τ_w is

$$0{\cdot}764 \times 33 + 0{\cdot}236 \times 18 \doteqdot 30\%,$$

which is quite low. However, if the height h is altered to 0·010 in., then the pressure rise becomes 0·28 in. Hg, which can be measured to an accuracy of about 14%. Hence the accuracy of τ_w is

$$0{\cdot}764 \times 14 + 0{\cdot}236 \times 10 \doteqdot 13\%.$$

This suggests that the height h of the surface pitot should be chosen for the particular test being carried out. For low Mach numbers or high Reynolds numbers tube heights of the order of 0·005 in. will be adequate, but for high Mach numbers or low Reynolds numbers tube heights of about 0·010 in. or larger will be needed to give reasonable accuracy. There may be additional errors due to inaccuracy of the calibration curve (*see* Section 5.4).

7. *Skin Friction on a Slender Delta Wing.*

As a preliminary test of surface pitot tubes, the skin friction was measured on a slender delta wing to which 13 tubes were attached. All the tubes were attached with their leading edges normal to the model centreline. There was no noticeable increase in the time lag of the pressure readings. Due to faulty instrumentation, pressures were not recorded for certain Mach numbers and incidences of the model. However, enough information was obtained to enable a few deductions to be made.

The model (Fig. 9) was a delta wing of aspect ratio 4/3, having a Lord V area distribution[1], with diamond cross sections and a root thickness-chord ratio of 11·2%, the root chord being 5 ft. The surface pitot tubes were placed at the positions shown on Fig. 9. Results were obtained for the following combinations of Mach number M, Reynolds number Re per foot, and incidence α.

M	Re per foot	α
1·6	2×10^6	$-4°, -2°, 0°, +2°, +4°$
2·0	2×10^6	$-4°, -2°, 0°, +2°$
2·0	1×10^6	$0°$
2·2	2×10^6	$0°$
2·4	2×10^6	$-10°, -8°, -6°, -4°, +6°, +8°, +10°$
2·6	2×10^6	$0°$.

A positive incidence indicates that the skin friction was measured on the suction side of the wing. The skin friction was evaluated as described in Section 6, and the results interpreted as skin-friction coefficients relative to free-stream conditions. No attempt was made to fix transition on the wing, so that some regions of laminar flow exist. Pressure distributions measured in other tests are shown in Fig. 10.

The results for a Mach number of 1·6, showing the effect of variation of incidence, are given in Fig. 11 for the two spanwise positions $y/s = 0{\cdot}05$ and $0{\cdot}40$, y being the spanwise distance from the root and s the semi-span of the wing. From the results for $y/s = 0{\cdot}05$, it is clear that the most forward surface pitot tube is in a region of laminar flow. The skin-friction coefficient for this point is not accurate since no calibration has been made in a laminar boundary layer. The remaining two surface pitot tubes, at $y/s = 0{\cdot}25$ and $0{\cdot}59$, for which results are not given, were in regions of laminar flow for most of the tests, and it is not considered worth while quoting any results for these. The results for variation of incidence at Mach numbers of 2·0 and 2·4 are shown in Figs. 12 and 13 respectively. The effect of Mach number on the skin friction is shown in Fig. 14, which gives the results for all Mach numbers at zero incidence. The effect of Reynolds number is shown in Fig. 15, which gives the results for a Mach number of 2·0 at zero incidence for the two Reynolds numbers used.

From Figs. 11, 12 and 13 it is seen that, for moderate incidences, the skin friction is increased on the pressure side of the wing and decreased on the suction side. This effect is partly due to the variation of local kinetic pressure with incidence. In Fig. 16, the results for $M = 2{\cdot}4$ are plotted as skin-friction coefficients relative to local kinetic pressure, and some reduction in the spread of the curves is obtained.

The only results for high incidences are those for $M = 2{\cdot}4$ (Fig. 13), where, unfortunately, results for zero incidence are not available. At the highest incidence ($+10°$), for $y/s = 0{\cdot}05$, the skin friction increases towards the rear of the model, instead of falling as would be expected. For $y/s = 0{\cdot}40$, for the same incidence, the skin friction was too small to be measured for the upstream four surface pitot tubes. This can be explained if the reattachment line of the flow separating from the leading edge was aft of all but the downstream tube. No explanation is offered for the behaviour of the skin friction for $y/s = 0{\cdot}05$.

Fig. 14 shows the effect of Mach number on the skin friction at zero incidence. It is seen that the skin-friction coefficient decreases as the Mach number increases, as would be expected. From flow visualisation it is known that the transition Reynolds number is about 2 million for the section $y/s = 0{\cdot}05$, and about 1 million for $y/s = 0{\cdot}40$. These figures agree quite well with the form of the skin-friction curves obtained. The theoretical curves shown on Fig. 14 were obtained by assuming that the pressure gradients on the wing had a negligible effect on the skin friction. They agree moderately well with measurements over the forward part of the wing, but are significantly higher over the rear portion. This may be due to three-dimensional effects in the boundary layer. From the theoretical work of Lord and Brebner[1] it can be shown that the streamlines over the rear portion of a wing with Lord V area distribution are converging. While this wing is rather thick for linearised theory to be accurate, this behaviour is probably not qualitatively different. This would tend to increase the boundary-layer thickness and decrease the skin friction, in agreement with the measured values.

The effect of varying Reynolds number at $M = 2{\cdot}0$ and zero incidence is shown in Fig. 15. As expected the skin-friction coefficients are higher for lower Reynolds number. Again the measured

values agree moderately well with flat-plate values over the forward portion of the wing, but are lower over the rear portion of the wing. It is worth pointing out that the surface pitot tube at $x/c_0 = 0{\cdot}60$, $y/s = 0{\cdot}40$ appears to lie in the transition region for a Reynolds number of 1 million per foot. The shape of the skin-friction curve through transition can in this case therefore be roughly defined. The length of the region corresponds to a Reynolds number of about 1 million which is not inconsistent with zero-pressure-gradient results at low speeds. For example the profiles given by Schubauer and Klebanoff in Fig. 3 of Ref. 33 imply a Reynolds number for the transition region of $1{\cdot}1$ million.

8. *Skin Friction on a Biconvex Cone.*

Another example of the application of surface pitot tubes is a brief investigation at a Mach number of 2 and Reynolds number per foot of $3{\cdot}3 \times 10^6$ of the skin friction on the biconvex cone shown in Fig. 17. This model is one of a series on which pressure measurements have been described by Britton[34]. Surface-pitot measurements were made at a spanwise station on one surface at 73% root chord from the apex, over an incidence range of ± 16 degrees. Pressure coefficients extracted from Ref. 34 are shown in Fig. 18. The pressure distributions at incidence are characteristic of the separated-flow conditions found on slender wings with subsonic leading edges. (The aerodynamic slenderness parameter of the tests was $0{\cdot}43$.) From the distributions it can be seen that a vortex has formed at an incidence as low as 4 degrees and that at 16 degrees the three peaks in the suction on the upper surface imply the existence of three vortices. The surface flow on the upper surface (i.e. for positive incidence) will thus contain large variations in direction, and measurements with the surface pitot tubes, which were set with the leading edges normal to the model centreline, will be subject to errors. Unfortunately shortage of time prevented the taking of any surface oil-flow observations and so corrections to the measurements cannot be estimated. However, Fig. 7 shows that the error in surface shear would be not more than 10% for 20 degrees flow deviation.

The local skin-friction coefficients as deduced from the surface-pitot-tube readings are shown in Fig. 19 in terms of free-stream kinetic pressure and in Fig. 20 in terms of local kinetic pressure. The local kinetic pressure was calculated from the pressure coefficients of Fig. 18 assuming the flow to be isentropic. This assumption will be inaccurate for large incidences because of shock losses and viscous losses associated with vortices. The variation of skin friction with incidence is appreciably reduced by basing the coefficients on local kinetic pressure.

Considering first the lower surface {Fig. 20(b)} the general shape of the curves at small incidence is consistent with the transition line usually found on slender wings (but not established for this model) where the transition on the centreline takes place at a higher Reynolds number than elsewhere. Such a pattern would give high local turbulent skin-friction coefficients on the centreline corresponding to an effectively lower Reynolds number and low values for the most outboard position if this were in the laminar or transition region. The magnitude of the measured skin friction is compared with flat-plate estimates, i.e. assuming the flow to be everywhere chordwise at two Mach numbers $1{\cdot}6$ and $1{\cdot}93$. These Mach numbers correspond to the pressure coefficients on the model centreline at -16 degrees and zero incidence respectively. Apart from the centreline the measurements at low incidence are everywhere lower than the estimate, and fall more sharply between $y/s = 0{\cdot}8$ and $0{\cdot}6$. This behaviour might be due to the inflow implied by the pressure distributions of Fig. 18. The inflow will have two opposite effects, a reduction of effective local Reynolds number (and

consequent increase in skin friction) because the streamline at a given spanwise station will start from the leading edge outboard of the station, and a reduction in skin friction because of the convergence of the streamlines. With increasing incidence the skin friction increases rapidly up to 12 degrees but then decreases at 16 degrees incidence. The increase up to 12 degrees may be associated with an aft movement of transition together with the effect of diverging streamlines which the pressure coefficients indicate. The behaviour at 16 degrees incidence is not understood.

On the upper surface {Figs. 19(a) and 20(a)} the distribution is much more irregular showing the peaks and troughs which would be expected at the reattachment and separation lines occurring in the surface flow. In the absence of surface flow pictures an estimate of the positions of the reattachment lines with incidence has been made. Marsden, Simpson and Rainbird[35] have studied the separated flow over delta wings at low speeds and from their results it is possible to correlate the spanwise position of the reattachment lines with the spanwise position of the peak suction. This is shown in Fig. 21 plotted against the incidence parameter α/K where K is the tangent of half the wing apex angle. This line and Fig. 18 were used to produce the dotted curve in Fig. 22 which is compared with the peak skin-friction values. There are insufficient skin-friction measurements to define the peaks clearly and their positions are indicated by lines rather than points. All the measurements are outboard of the estimate. This outboard movement is probably a Mach number effect. The spanwise positions of peak suction and vortex core are approximately the same and so Fig. 21 may be taken to be the ratio of span of reattachment lines to vortex span. Now for a given vortex span the vortices are much closer to the wings at supersonic speeds than at low speeds (*see*, for example, Gaudet and Winter[36]) and consequently the attachment lines at supersonic speeds may be farther outboard in relation to the vortices than at low speeds.*

Further work is needed to establish more accurately the peak skin-friction values and positions, and the surface flow. It might, however, be remarked that the large variations in skin friction measured imply by Reynolds analogy large variations in heat-transfer rates and consequent possible structural problems for an aircraft operating with this type of flow.

9. *Conclusions.*

It has been shown that surface pitot tubes offer a simple way of measuring the surface shearing stress in turbulent boundary layers at supersonic speeds. The surface pitot tubes used were formed by cementing pieces of razor blade to surfaces with the chamfered edges overlapping static-pressure holes. Tests over a range of Mach numbers and Reynolds numbers have shown that a correlation of the same form as that used by Preston[16] can be obtained, without introducing Mach number as an additional parameter. Fig. 5 shows the correlation obtained.

Some tests have been made on the effect of yaw on the surface pitot tubes, and a correlation is suggested for relating the results to those at zero yaw.

The technique has been applied to two models in the 8 ft × 8 ft Tunnel at R.A.E., Bedford, over a range of Mach numbers, Reynolds numbers and incidences. Regions of laminar flow were readily detected, and the variation of skin-friction coefficients with Mach number and Reynolds number agreed qualitatively with the variation of skin friction on a flat plate.

---

* Recent work by Wyatt in a low-speed tunnel on a rhombic cone has shown the reattachment line to be inboard of the peak-skin-friction line.

The technique used here is applicable to any model designed for pressure-plotting tests. The pieces of razor blade used to form the surface pitot tubes can be removed easily so restoring the model surface to its original condition.

Further tests of surface pitot tubes of the type used here, over a wider range of Mach numbers, Reynolds numbers and tube heights, and in laminar and transitional boundary layers, are needed to extend the range of applicability.

LIST OF SYMBOLS

c_0	Root chord of wing
C_F	Mean skin-friction coefficient
c_f	Local skin-friction coefficient
c_p	Pressure coefficient
h	Height of surface pitot tube
K	Tangent of half the wing apex angle
M	Mach number
Re	Reynolds number
s	Semi-span of wing
T	Temperature
U	Mean velocity in boundary layer
U_s	Velocity defined by $\Delta P = \frac{1}{2}\rho_w U_s^2$
u_τ =	$(\tau_w/\rho_w)^{1/2}$
x	Distance from effective beginning of turbulent boundary layer, or from apex of wing
y	Distance from centreline of wing
α	Angle of incidence
β	Angle of yaw
ΔP	Surface pitot pressure—local static pressure
θ	Momentum thickness of boundary layer
μ	Viscosity
ν	Kinematic viscosity
ρ	Density
τ	Shearing stress

Subscripts

1	Free-stream conditions
w	Wall conditions

Superscripts

*	Intermediate enthalpy conditions

REFERENCES

No.	Author(s)	Title, etc.
1	W. T. Lord and G. G. Brebner ..	Supersonic flow past slender pointed wings with 'similar' cross sections at zero lift. *Aero. Quart.*, Vol. 10, pp. 79 to 102. 1959.
2	A. O. Ormerod and T. Sprinks ..	Measurements of lift, drag and pitching moment on a delta wing of aspect ratio 2/3 at Mach numbers of 1·34, 1·59 and 1·79. R.A.E. Tech. Note Aero. 2553. A.R.C. 20,348. March, 1958.
3	W. R. Sears	Boundary layers in three dimensional flow. *App. Mech. Rev.*, Vol. 7, pp. 281 to 285. 1954.
4	F. K. Moore	Three dimensional boundary layer theory. *Advances in Applied Mechanics*, Vol. IV, pp. 159 to 228. Academic Press, New York. 1956.
5	J. C. Cooke and M. G. Hall ..	Boundary layers in three dimensions. *Progress in Aeronautical Sciences*, Vol. 2, pp. 221 to 282. Pergamon Press. 1962.
6	G. B. Schubauer and P. S. Klebanoff	Investigation of separation of the turbulent boundary layer. N.A.C.A. Report 1030. 1951.
7	von G. Kempf	Weitere Reigungsergebnisse an ebenen glatten und rauhen Flächen. *Hydrodynamische Probleme des Schiffsantriebs*, Vol. 1, pp. 74 to 82. 1932.
8	S. Dhawan	Direct measurements of skin friction. N.A.C.A. Report 1121. 1953.
9	D. W. Smith and J. H. Walker ..	Skin-friction measurements in incompressible flow. N.A.S.A. Tech. Report R-26. 1959.
10	H. Ludwieg	Instrument for measuring the wall shearing stress of turbulent boundary layers. N.A.C.A. Tech. Memo. 1284. May, 1950.
11	H. W. Liepmann and G. T. Skinner	Shearing-stress measurements by use of a heated element. N.A.C.A. Tech. Note 3268. November, 1954.
12	N. S. Diaconis	The calculation of wall-shearing stress from heat transfer measurements in compressible flows. *J. Ae. Sci.*, Vol. 21, pp. 201 and 202. 1954.
13	H. Ludwieg and W. Tillmann ..	Investigations of the wall-shearing stress in turbulent boundary layers. N.A.C.A. Tech. Memo. 1285. A.R.C. 14,800. May, 1950.
14	T. E. Stanton, D. Marshall and C. N. Bryant.	On the conditions at the boundary of a fluid in turbulent motion. *Proc. Roy. Soc.* A, Vol. 97, pp. 413 to 434. 1920.

(88675)

No.	*Author(s)*	*Title, etc.*
15	A. Fage and V. M. Falkner ..	An experimental determination of the intensity of friction on the surface of an aerofoil. *Proc. Roy. Soc.* A, Vol. 129, pp. 378 to 410. 1930.
16	J. H. Preston	The determination of turbulent skin friction by means of pitot tubes. *J. R. Ae. Soc.*, Vol. 58, pp. 109 to 121. 1954.
17	J. N. Hool	Measurement of skin friction using surface tubes. *Aircraft Engineering*, Vol. 28, pp. 52 to 54. 1956.
18	R. J. Monaghan and J. R. Cooke ..	The measurement of heat transfer and skin friction at supersonic speeds. Part IV. Tests on a flat plate at $M = 2{\cdot}82$. A.R.C. C.P. 140. June, 1952.
19	G. I. Taylor	Measurements with a half pitot tube. *Proc. Roy. Soc.* A, Vol. 166, pp. 476 to 481. 1938.
20	L. Trilling and R. J. Hakkinen ..	The calibration of the Stanton tube as a skin friction meter. 50 *Jahre Grenzschichtforschung*, pp. 201 to 209. Friedr. Vieweg und Sohn, Braunschweig. 1955.
21	E. F. Relf, R. C. Pankhurst and W. S. Walker.	The use of pitot tubes to measure skin friction on a flat plate. A.R.C. 17,025. August, 1954. (Subsequently included in R. & M. 3185.)
22	E. Y. Hsu	The measurement of local turbulent skin friction by means of surface pitot tubes. David Taylor Model Basin, Report 957. 1955.
23	F. W. Fenter and C. J. Stalmach ..	The measurement of local turbulent skin friction at supersonic speeds by means of surface impact pressure probes. Defense Research Laboratory, University of Texas, Report DRL-392. 1957.
24	P. Bradshaw and N. Gregory ..	The determination of local turbulent skin friction from observations in the viscous sub-layer. A.R.C. R. & M. 3202. March, 1959.
25	S. S. Abarbanel, R. J. Hakkinen and L. Trilling.	Use of a Stanton tube for skin-friction measurements. N.A.S.A. Memo. 2-17-59W. TIL 6275. March, 1959.
26	A. Thom	The flow at the mouth of a Stanton pitot. A.R.C. R. & M. 2984. October, 1952.
27	G. E. Gadd	A note on the theory of the Stanton tube. A.R.C. R. & M. 3147. October, 1958.
28	R. J. Monaghan and J. E. Johnson ..	The measurement of heat transfer and skin friction at supersonic speeds. Part II. Boundary layer measurements on a flat plate at $M = 2{\cdot}5$ and zero heat transfer. A.R.C. C.P. 64. December, 1949.

REFERENCES—*continued*

No.	*Author(s)*	*Title, etc.*
29	R. J. Monaghan	Formulae and approximations for aerodynamic heating rates in high speed flight. A.R.C. C.P. 360. October, 1955.
30	A. E. Stevens	A wind tunnel investigation at $M = 1 \cdot 93$ of the pressure drag of some surface irregularities. English Electric G.W. Division, Report LA.t.081. 1958.
31	A. E. Stevens	A wind tunnel investigation at supersonic speeds of the pressure drag of a two-dimensional step. English Electric G.W. Division, Report LA.t.082. 1959.
32	R. A. Granville and G. Boxall ..	Measurement of convective heat transfer by means of the Reynolds analogy. *Brit. J. App. Phys.*, Vol. 11, pp. 471 to 475. 1960.
33	G. B. Schubauer and P. S. Klebanoff	Contributions on the mechanics of boundary-layer transition. A.R.C. 17,969. September, 1955. N.A.C.A. Report 1289. 1956.
34	J. W. Britton	Pressure measurements at supersonic speeds on three uncambered conical wings of unit aspect ratio. A.R.C. C.P. 641. May, 1962.
35	D. J. Marsden, R. W. Simpson and W. J. Rainbird.	The flow over delta wings at low speeds with leading edge separation. C. of A. Report 114. A.R.C. 20,409. February, 1958.
36	L. Gaudet and K. G. Winter ..	Preliminary measurements of the flow field on the leeside of a delta wing of unit aspect ratio at a Mach number of 2·6 and an incidence of 15°. R.A.E. Tech. Note Aero. 2787. A.R.C. 23,510. September, 1961.

TABLE 1

Characteristics of Boundary Layer, 9 in. × 8 in. Tunnel

Upstream position

H_0 (in. Hg)	θ (in.)	δ^* (in.)	H	c_f
65·2	0·0328	0·0997	3·04	0·00160
40·0	0·0353	0·1208	3·42	0·00172
32·6	0·0360	0·1147	3·18	0·00180
20·0	0·0397	0·1251	3·15	0·00195
16·3	0·0412	0·1291	3·14	0·00201

Centre position

H_0 (in. Hg)	θ (in.)	δ^* (in.)	H	c_f
65·2	0·0339	0·1062	3·13	0·00158
40·0	0·0369	0·1039	2·82	0·00170
32·6	0·0386	0·1187	3·08	0·00175
20·0	0·0424	0·1322	3·12	0·00189
16·3	0·0445	0·1382	3·10	0·00195

Downstream position

H_0 (in. Hg)	θ (in.)	δ^* (in.)	H	c_f
65·2	0·0367	0·1129	3·08	0·00151
40·0	0·0397	0·1234	3·11	0·00165
32·6	0·0413	0·1275	3·09	0·00170
16·3	0·0467	0·1451	3·11	0·00193

TABLE 2

Characteristics of Boundary Layer, 13 in. Tunnel

Centreline position

M	θ (in.)	δ^* (in.)	H	c_f
2·70	0·0542	0·2354	4·34	0·00146
2·52	0·0506	0·1989	3·93	0·00153
2·34	0·0488	0·1709	3·50	0·00161
2·16	0·0484	0·1566	3·24	0·00164
1·96	0·0496	0·1436	2·90	0·00172
1·77	0·0512	0·1334	2·61	0·00179

Position above centreline

M	θ (in.)	δ^* (in.)	H	c_f
2·70	0·0480	0·1955	4·07	0·00150
2·52	0·0471	0·1742	3·70	0·00156
2·34	0·0479	0·1672	3·49	0·00160
2·15	0·0479	0·1534	3·20	0·00166
1·97	0·0500	0·1452	2·90	0·00172
1·77	0·0536	0·1392	2·60	0·00177

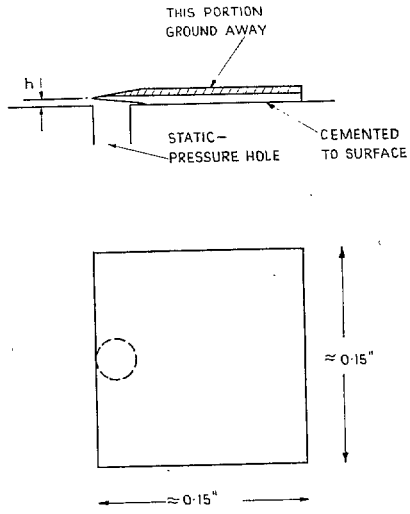

FIG. 1. Type of surface pitot tube used.

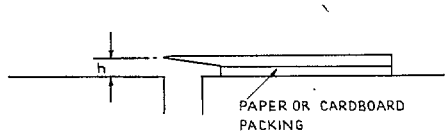

FIG. 2. Method of varying height of surface pitot tube.

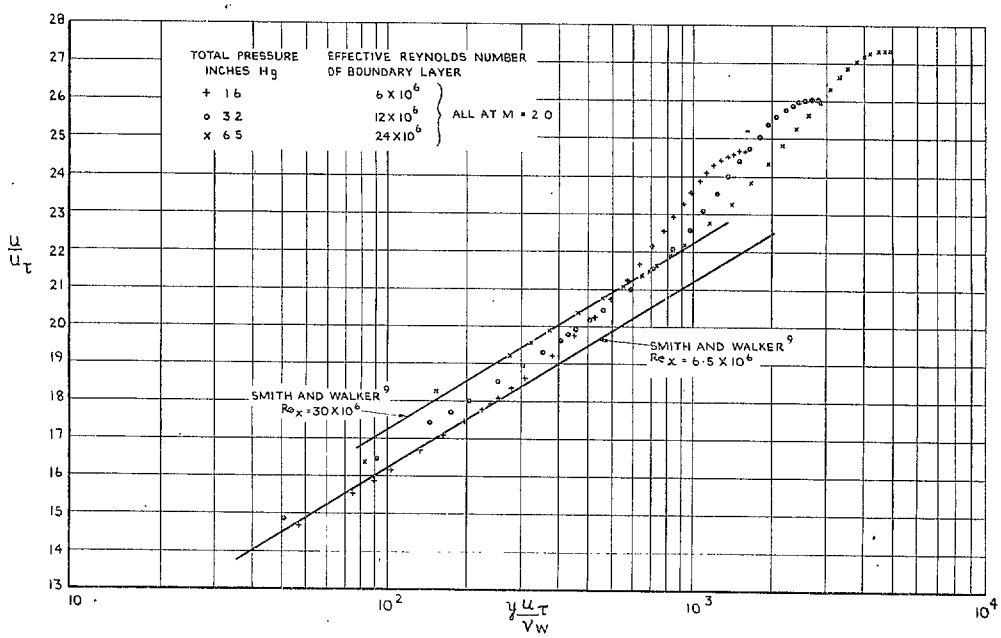

FIG. 3. Boundary-layer profiles, 9 in. × 8 in. Tunnel.

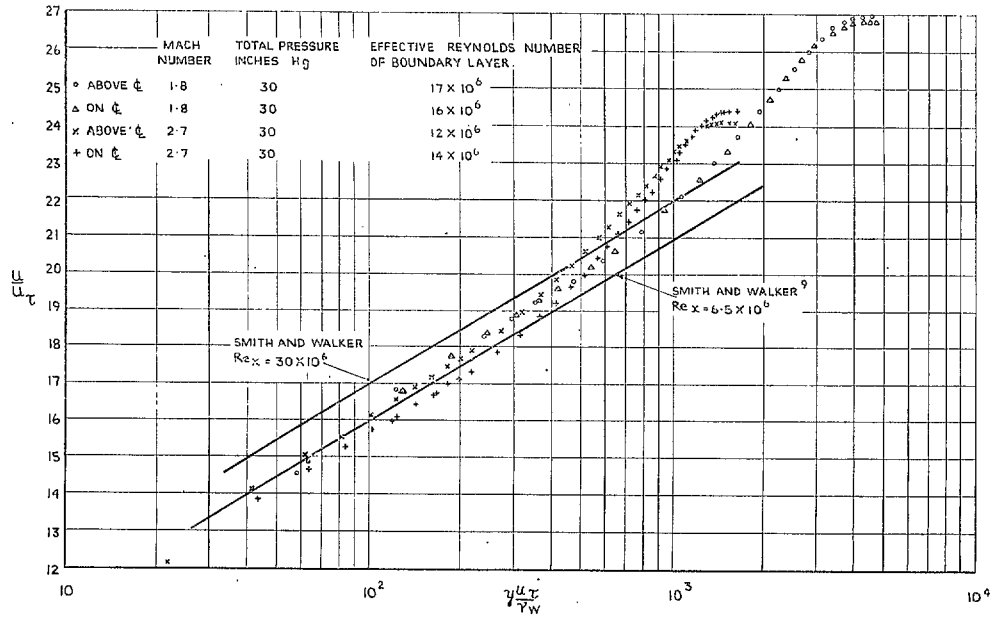

FIG. 4. Boundary-layer profiles, 13 in. Tunnel.

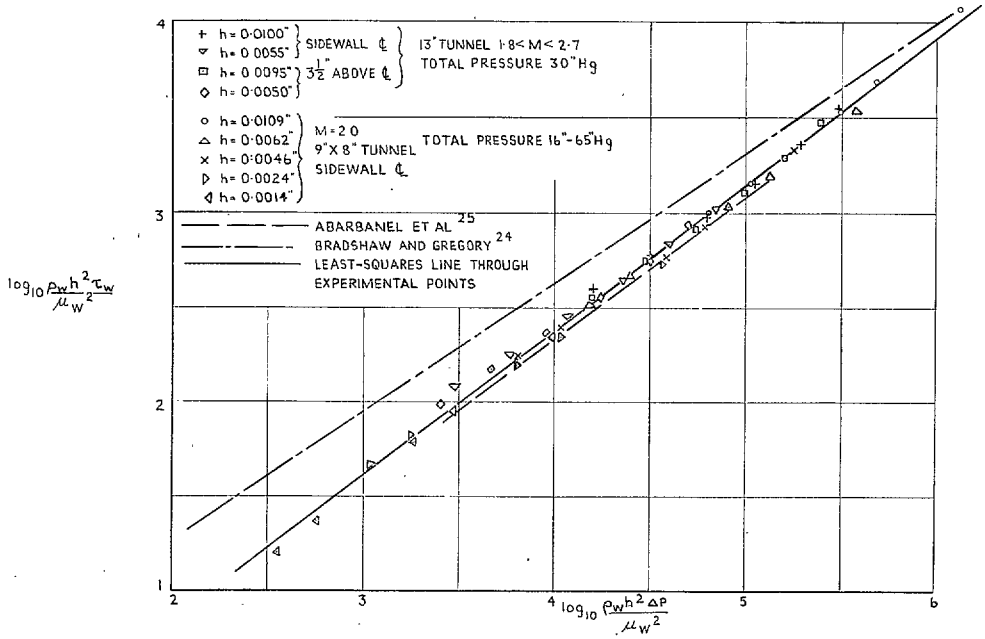

FIG. 5. Surface-pitot-tube-calibration in 9 in. × 8 in. and 13 in. Wind Tunnels.

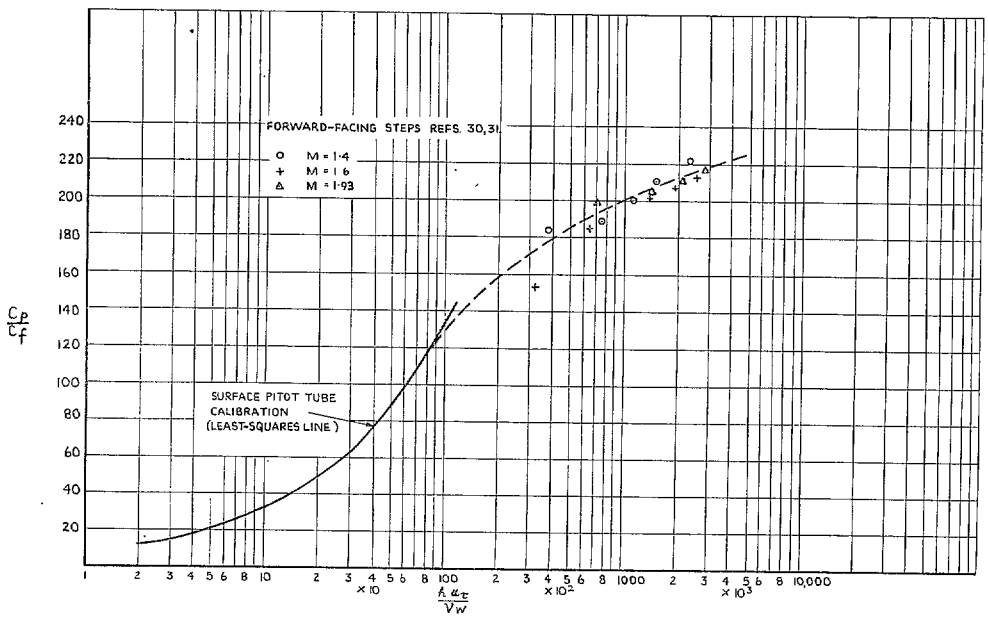

FIG. 6. Comparison between surface-pitot-tube calibration and pressure coefficients on steps.

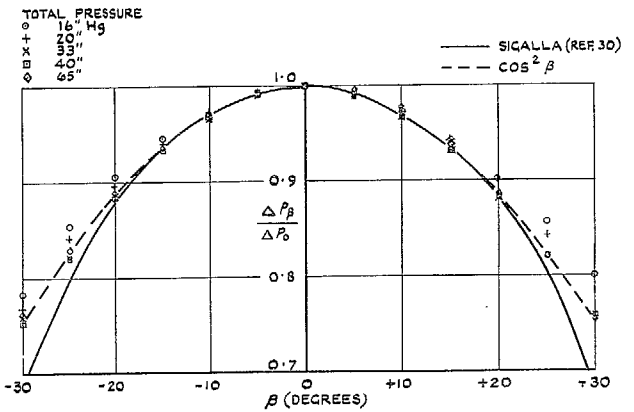

FIG. 7. Effect of yaw on pressure rise measured by surface pitot tube.

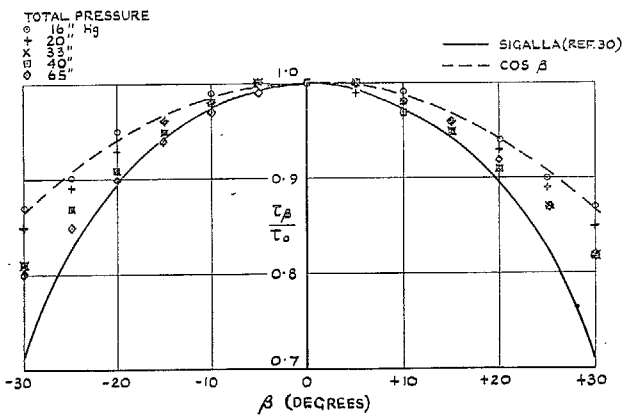

FIG. 8. Effect of yaw on skin friction deduced from surface-pitot-tube reading.

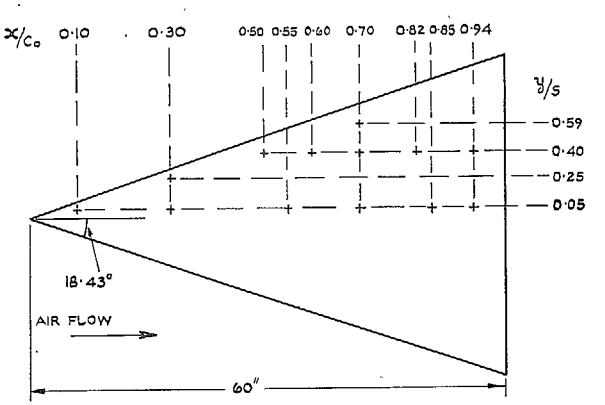

(a) POSITION OF SURFACE PITOT TUBES

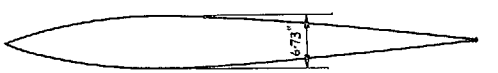

(b) ROOT SECTION

FIG. 9. Slender delta wing.

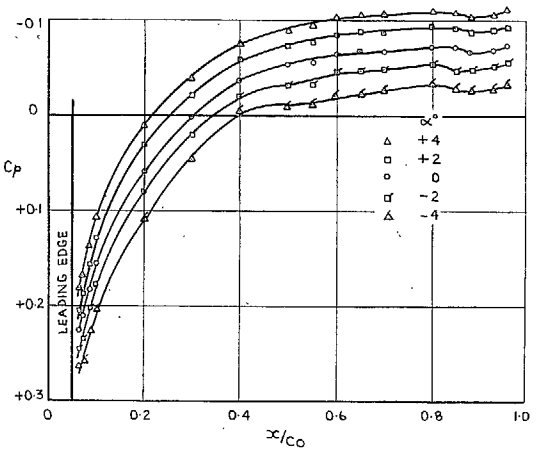

(a) $y/s = 0{\cdot}05$, M=1·6.

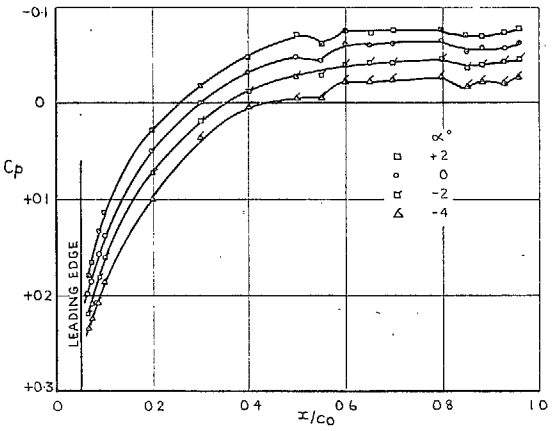

(c) $y/s = 0{\cdot}05$, M = 2·0.

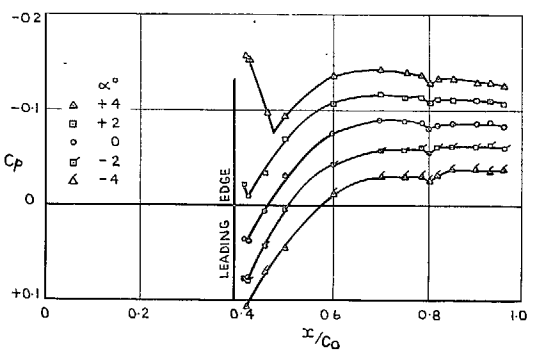

(b) $y/s = 0{\cdot}40$, M=1·6.

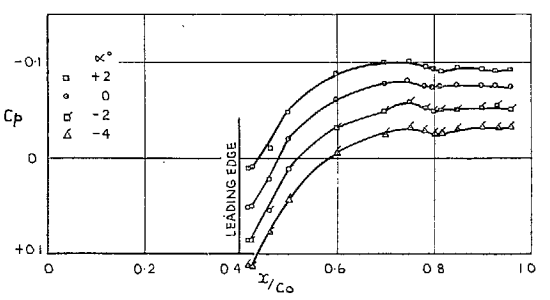

(d) $y/s = 0{\cdot}40$, M = 2·0.

FIG. 10. Static-pressure distributions on slender delta wing.

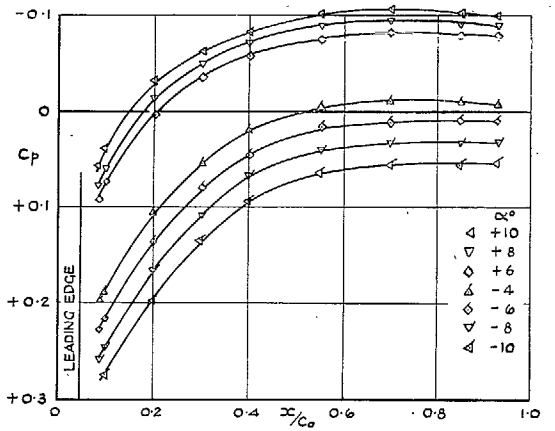

(e) $y/s = 0·05$, M = 2·4.

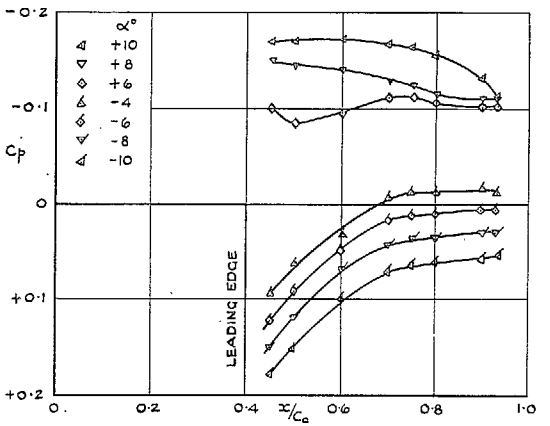

(f) $y/s = 0·40$, M = 2·4.

FIG. 10 (*continued*). Static-pressure distributions on slender delta wing.

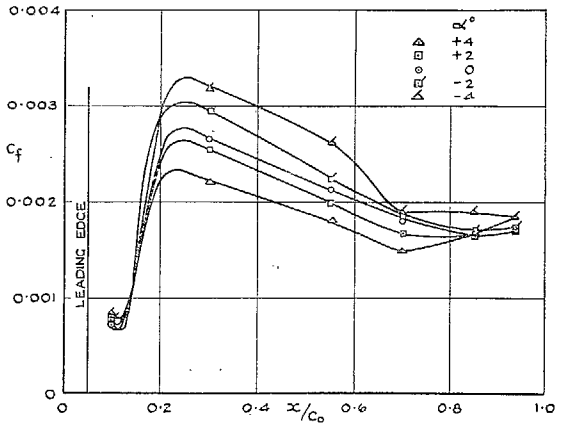

(a) $y/s = 0·05$

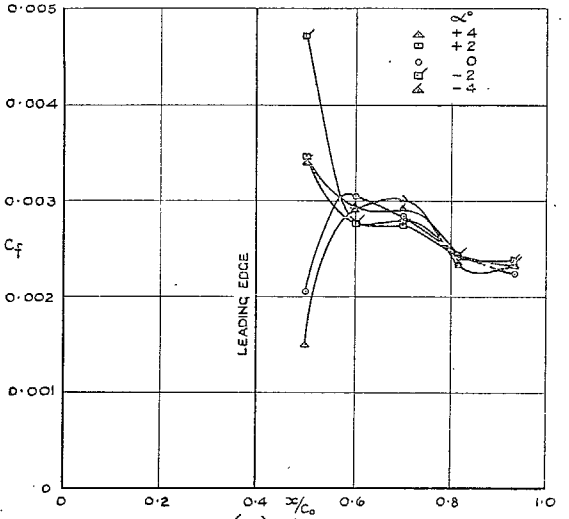

(b) $y/s = 0·40$

FIG. 11. Effect of incidence on skin-friction coefficients on slender delta wing (referred to free-stream kinetic pressure) $M = 1·6$, $Re = 2 \times 10^6$/ft.

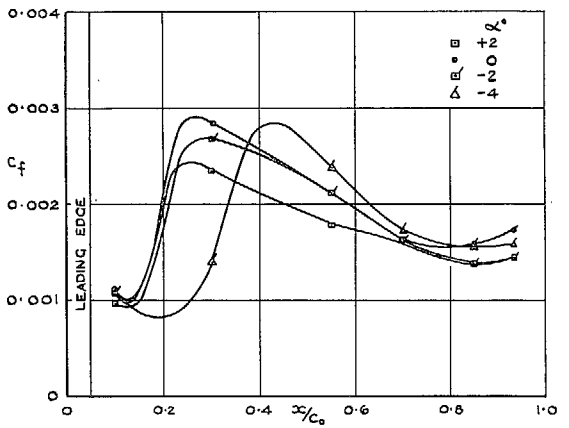

(a) $y/s = 0{\cdot}05$

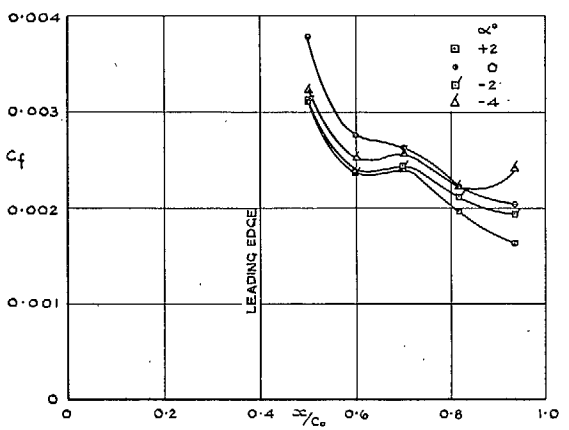

(b) $y/s = 0{\cdot}40$

FIG. 12. Effect of incidence on skin-friction coefficients on slender delta wing (referred to free-stream kinetic pressure) $M = 2{\cdot}0$, $Re = 2 \times 10^6$/ft.

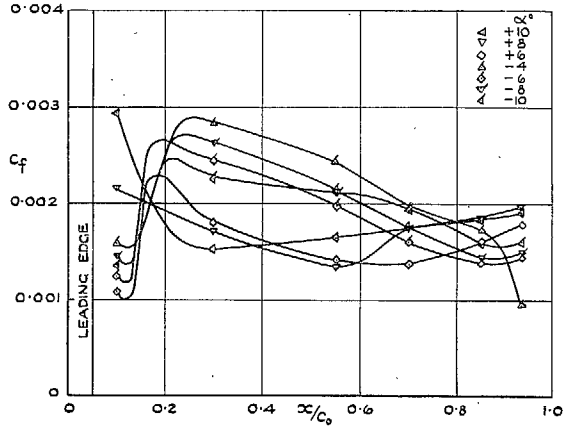

(a) $y/s = 0{\cdot}05$

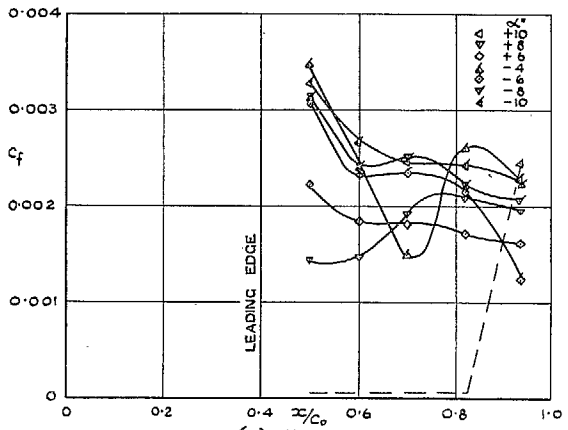

(b) $y/s = 0{\cdot}40$

FIG. 13. Effect of incidence on skin-friction coefficients on slender delta wing (referred to free-stream kinetic pressure) $M = 2{\cdot}4$, $Re = 2 \times 10^6$/ft.

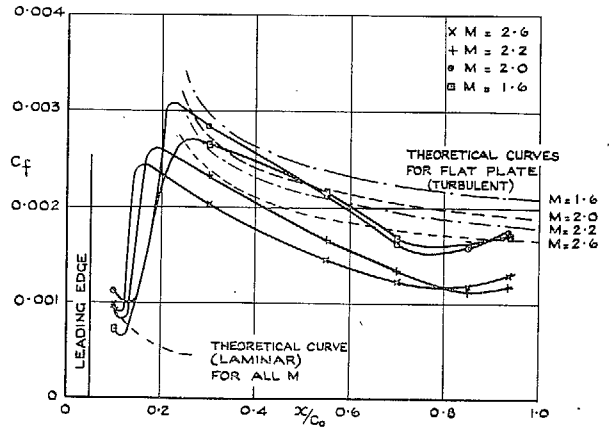

(a) $y/s = 0{\cdot}05$

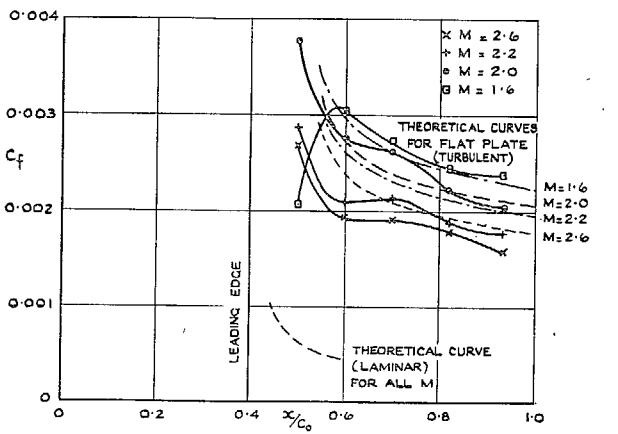

(b) $y/s = 0{\cdot}40$

FIG. 14. Effect of Mach number on skin-friction coefficients on slender delta wing at zero incidence (referred to free-stream kinetic pressure) $Re = 2 \times 10^6$/ft.

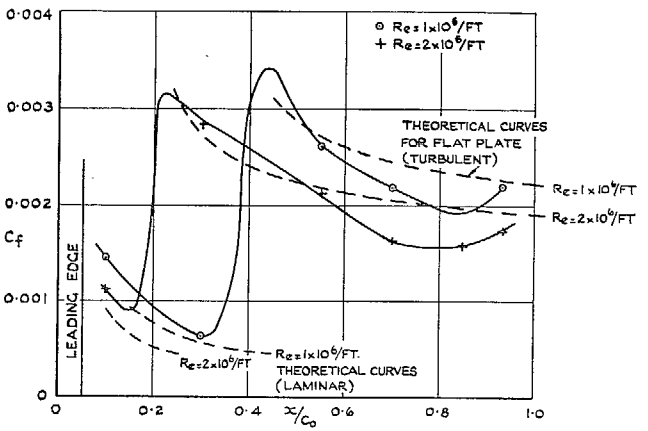

(a) $y/s = 0{\cdot}05$

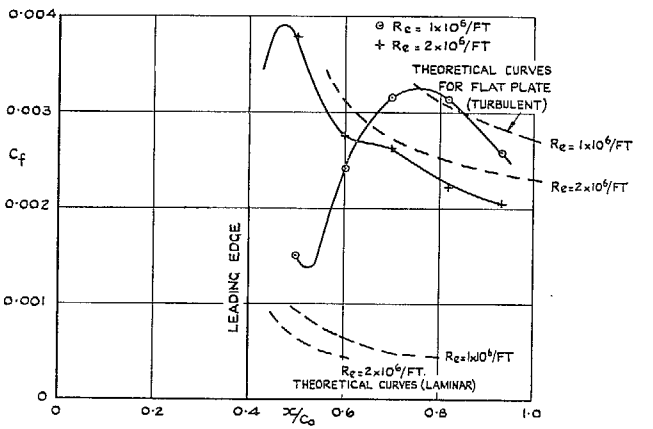

(b) $y/s = 0{\cdot}40$

FIG. 15. Effect of Reynolds number on skin-friction coefficients on slender delta wing at zero incidence (referred to free-stream kinetic pressure) $M = 2{\cdot}0$.

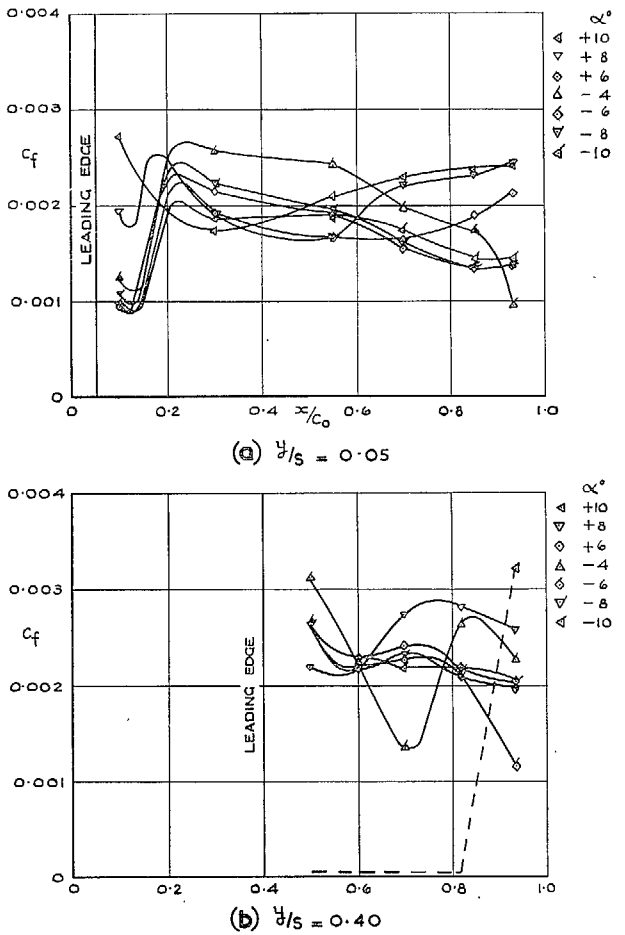

FIG. 16. Effect of incidence on skin-friction coefficients on slender delta wing (referred to local kinetic pressure) $M = 2·4$, $Re = 2 \times 10^6$/ft.

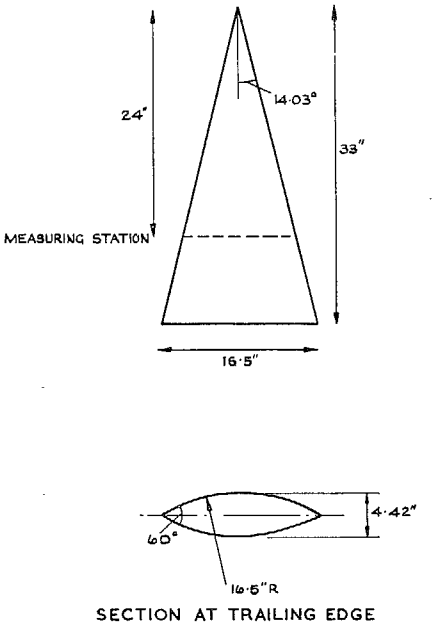

FIG. 17. Biconvex cone.

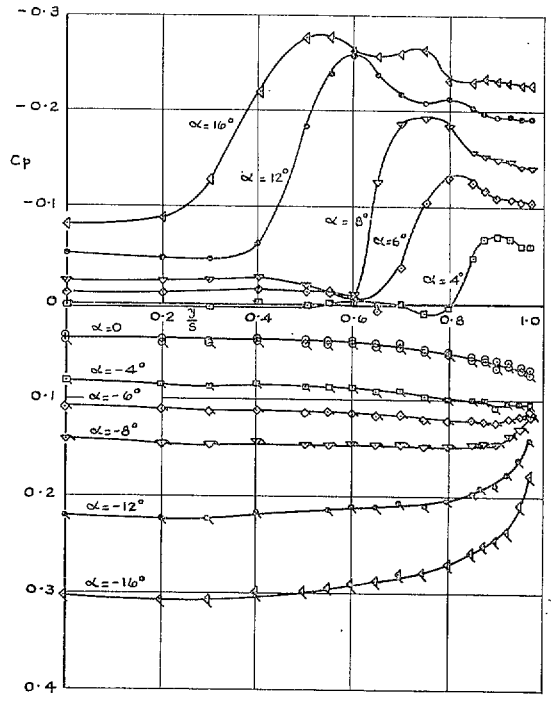

FIG. 18. Static-pressure distribution on biconvex cone $M = 2{\cdot}0$, $Re = 3{\cdot}3 \times 10^6$/ft.

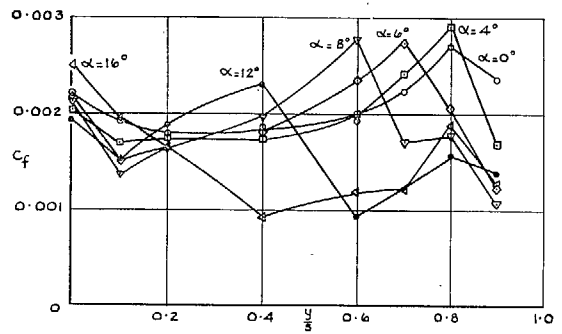

(a) POSITIVE INCIDENCE

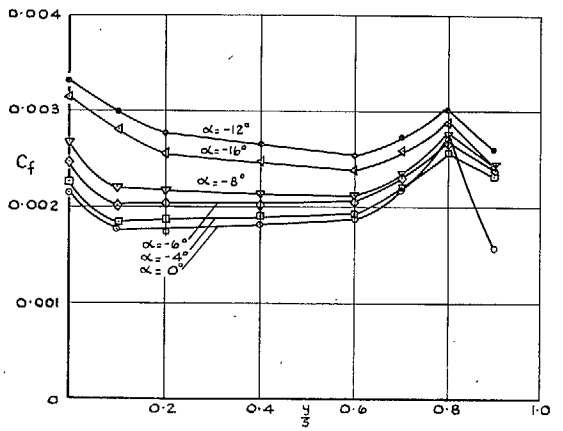

(b) NEGATIVE INCIDENCE

FIG. 19. Skin-friction coefficients on biconvex cone (referred to free-stream kinetic pressure) $M = 2{\cdot}0$, $Re = 3{\cdot}3 \times 10^6$/ft.

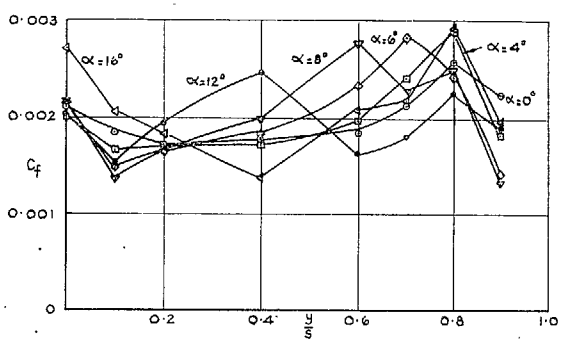

(a) POSITIVE INCIDENCE

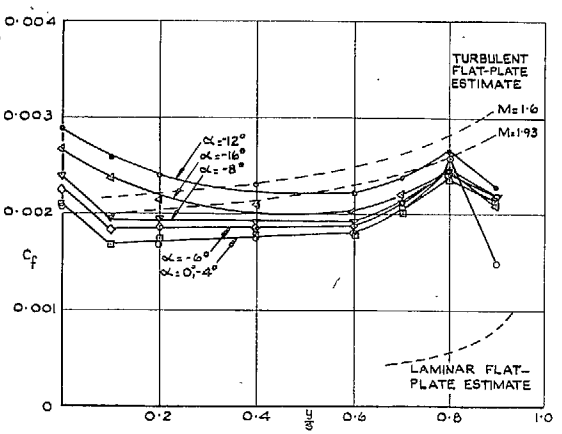

(b) NEGATIVE INCIDENCE

FIG. 20. Skin-friction coefficients on biconvex cone (referred to local kinetic pressure) $M = 2{\cdot}0$, $Re = 3{\cdot}3 \times 10^6$/ft.

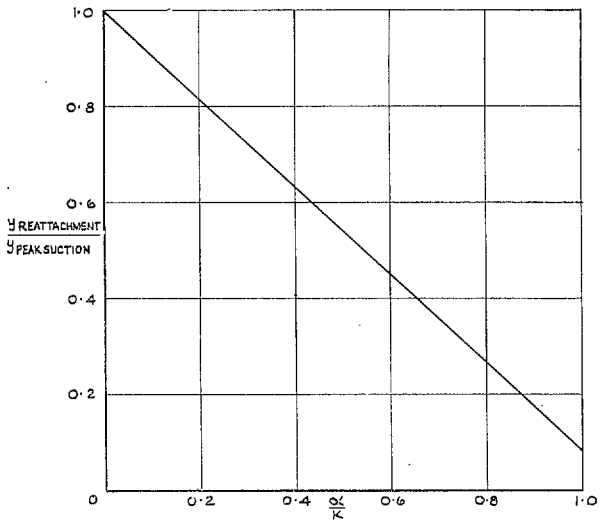

FIG. 21. Relationship between reattachment and peak-suction locations from Ref. 35.

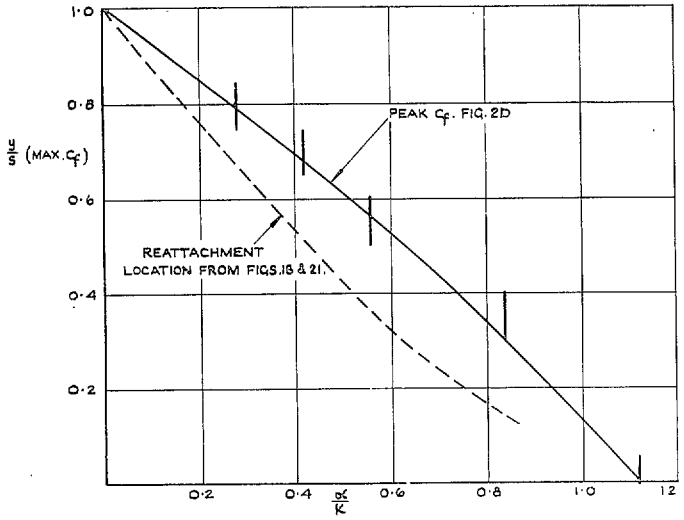

FIG. 22. Peak-skin-friction location, biconvex cone.

(88675) Wt. 65/1418 K.5 1/64 Hw.

Publications of the Aeronautical Research Council

ANNUAL TECHNICAL REPORTS OF THE AERONAUTICAL RESEARCH COUNCIL (BOUND VOLUMES)

1942 Vol. I. Aero and Hydrodynamics, Aerofoils, Airscrews, Engines. 75*s.* (post 2*s.* 9*d.*)
Vol. II. Noise, Parachutes, Stability and Control, Structures, Vibration, Wind Tunnels. 47*s.* 6*d.* (post 2*s.* 3*d.*)

1943 Vol. I. Aerodynamics, Aerofoils, Airscrews. 80*s.* (post 2*s.* 6*d.*)
Vol. II. Engines, Flutter, Materials, Parachutes, Performance, Stability and Control, Structures. 90*s.* (post 2*s.* 9*d.*)

1944 Vol. I. Aero and Hydrodynamics, Aerofoils, Aircraft, Airscrews, Controls. 84*s.* (post 3*s.*)
Vol. II. Flutter and Vibration, Materials, Miscellaneous, Navigation, Parachutes, Performance, Plates and Panels, Stability, Structures, Test Equipment, Wind Tunnels. 84*s.* (post 3*s.*)

1945 Vol. I. Aero and Hydrodynamics, Aerofoils. 130*s.* (post 3*s.* 6*d.*)
Vol. II. Aircraft, Airscrews, Controls. 130*s.* (post 3*s.* 6*d.*)
Vol. III. Flutter and Vibration, Instruments, Miscellaneous, Parachutes, Plates and Panels, Propulsion. 130*s.* (post 3*s.* 3*d.*)
Vol. IV. Stability, Structures, Wind Tunnels, Wind Tunnel Technique. 130*s.* (post 3*s.* 3*d.*)

1946 Vol. I. Accidents, Aerodynamics, Aerofoils and Hydrofoils. 168*s.* (post 3*s.* 9*d.*)
Vol. II. Airscrews, Cabin Cooling, Chemical Hazards, Controls, Flames, Flutter, Helicopters, Instruments and Instrumentation, Interference, Jets, Miscellaneous, Parachutes. 168*s.* (post 3*s.* 3*d.*)
Vol. III. Performance, Propulsion, Seaplanes, Stability, Structures, Wind Tunnels. 168*s.* (post 3*s.* 6*d.*)

1947 Vol. I. Aerodynamics, Aerofoils, Aircraft. 168*s.* (post 3*s.* 9*d.*)
Vol. II. Airscrews and Rotors, Controls, Flutter, Materials, Miscellaneous, Parachutes, Propulsion, Seaplanes, Stability, Structures, Take-off and Landing. 168*s.* (post 3*s.* 9*d.*)

1948 Vol. I. Aerodynamics, Aerofoils, Aircraft, Airscrews, Controls, Flutter and Vibration, Helicopters, Instruments, Propulsion, Seaplane, Stability, Structures, Wind Tunnels. 130*s.* (post 3*s.* 3*d.*)
Vol. II. Aerodynamics, Aerofoils, Aircraft, Airscrews, Controls, Flutter and Vibration, Helicopters, Instruments, Propulsion, Seaplane, Stability, Structures, Wind Tunnels. 110*s.* (post 3*s.* 3*d.*)

Special Volumes

Vol. I. Aero and Hydrodynamics, Aerofoils, Controls, Flutter, Kites, Parachutes, Performance, Propulsion, Stability. 126*s.* (post 3*s.*)
Vol. II. Aero and Hydrodynamics, Aerofoils, Airscrews, Controls, Flutter, Materials, Miscellaneous, Parachutes, Propulsion, Stability, Structures. 147*s.* (post 3*s.*)
Vol. III. Aero and Hydrodynamics, Aerofoils, Airscrews, Controls, Flutter, Kites, Miscellaneous, Parachutes, Propulsion, Seaplanes, Stability, Structures, Test Equipment. 189*s.* (post 3*s.* 9*d.*)

Reviews of the Aeronautical Research Council

1939–48 3*s.* (post 6*d.*) 1949–54 5*s.* (post 5*d.*)

Index to all Reports and Memoranda published in the Annual Technical Reports

1909–1947 R. & M. 2600 (out of print)

Indexes to the Reports and Memoranda of the Aeronautical Research Council

Between Nos. 2351–2449	R. & M. No. 2450	2*s.* (post 3*d.*)
Between Nos. 2451–2549	R. & M. No. 2550	2*s.* 6*d.* (post 3*d.*)
Between Nos. 2551–2649	R. & M. No. 2650	2*s.* 6*d.* (post 3*d.*)
Between Nos. 2651–2749	R. & M. No. 2750	2*s.* 6*d.* (post 3*d.*)
Between Nos. 2751–2849	R. & M. No. 2850	2*s.* 6*d.* (post 3*d.*)
Between Nos. 2851–2949	R. & M. No. 2950	3*s.* (post 3*d.*)
Between Nos. 2951–3049	R. & M. No. 3050	3*s.* 6*d.* (post 3*d.*)
Between Nos. 3051–3149	R. & M. No. 3150	3*s.* 6*d.* (post 3*d.*)

HER MAJESTY'S STATIONERY OFFICE

from the addresses overleaf

Printed and published by
HER MAJESTY'S STATIONERY OFFICE

To be purchased from
York House, Kingsway, London W.C.2
423 Oxford Street, London W.1
13A Castle Street, Edinburgh 2
109 St. Mary Street, Cardiff
39 King Street, Manchester 2
50 Fairfax Street, Bristol 1
35 Smallbrook, Ringway, Birmingham 5
80 Chichester Street, Belfast 1
or through any bookseller

Printed in England

S.O. Code No. 23-3351